

Comparison of Hydraulic-Burst and Ball-on-Ring Tests for Measuring Biaxial Strength

Anupa Simpatico,^{*,†} W. Roger Cannon,^{*} and M. John Matthewson^{*}

Rutgers University, Piscataway, New Jersey 08855-0909

The statistics of failure of the hydraulic-burst (HB) test were compared with those of the ball-on-ring (BOR) test. Polycrystalline Al₂O₃ tape-cast specimens, both square and circular, in two different sizes, were tested. Both the mean strengths and the Weibull moduli from the BOR tests were approximately twice the values from the HB tests. The area (volume) under stress is much larger for the HB test than the BOR test; therefore, the HB data can be considered as a low-probability-of-failure, low-strength tail of the BOR curve that has a lower Weibull modulus than the high-stress portion. Thus, BOR tests give a misleading picture of improvements in mechanical strength, because of changes in the fabrication and handling of substrates. However, previous observations that the incidence of edge and support failures was very high in the HB test were confirmed. Also, the apparent strength of the HB specimens was affected more strongly by size and shape than was that of the BOR specimens.

I. Introduction

CONSIDERABLE effort has been expended in developing biaxial-flexure¹⁻⁸ tests for ceramic plates and thin ceramic substrates. The two, most widely used tests are ball-on-ring (BOR) and ring-on-ring (ROR); however, hydraulic-burst (HB) tests also have received some attention.^{9,10} Most studies of the biaxial-strength test have concentrated on accurate determination of the maximum stress; however, more often, the usefulness of the tests is derived from the detection of the occasional worst flaw, rather than from the mean strength. Figure 1 compares both the tangential- and radial-stress distributions (σ_t and σ_r , respectively) for BOR, ROR (where the diameter of the loading ring is half that of the supporting ring), and HB tests. This figure clearly indicates that the stressed area is much larger in the ROR and HB tests than in the BOR test. Comparison between the BOR and HB/ROR tests is similar to comparing the testing of long and short lengths of optical fiber. In this case, the long optical fiber could be considered to reside in a low-strength tail of the short-optical-fiber strength distribution, in which case a different distribution of flaws (i.e., a lower Weibull modulus, m) is observed on the low-stress tail.¹¹ Thus, the ROR and HB tests could be used to examine the important, low-strength tail of the strength distribution for the BOR specimens. Furthermore, if a low-strength tail of a different slope on the Weibull plot exists, then the BOR test is a questionable test, even for comparison of specimen lots (unless the tested BOR volume is comparable to the stressed volume of the component in service).

The popularity of the BOR test originates from its ease of testing. Similarly, the ROR test is easy to use, which explains its widespread acceptance. Two criticisms have been leveled against ROR tests: imperfect contact with the loading ring, and contact stresses beneath the loading ring. The former can be solved with a flexible loading ring,¹² a piston-on-three-ball test, or using flatter specimens.⁵ Tensile contact stresses beneath and on the opposite side of the loading ring were calculated to be ~20% higher than the center stress. Furthermore, they exist in the region of highest stress. Moreover, a recent study by Adler and Mihora¹³ showed that, using a round steel loading ring, the stress may be 55% higher here than in the center. Nevertheless, they showed that the contact stress is not significant when using a low-modulus polymer ring (DelrinTM, Dupont, Wilmington, DE). They also showed, however, using improved finite-element (FEM) analysis, that the contact stress increases, relative to the center stress, as the disk becomes thinner. Previous studies that considered contact stresses all used disks that were >2 mm thick. To avoid the contact stresses from the loading ring on the thin substrate specimens (0.635 mm) that have been used in the present study, the HB test was chosen instead of the ROR test. However, no work has been performed to determine whether the ROR test would have been satisfactory.

One of the difficulties with the HB test that has not been addressed to date is the use of specimens with a square geometry, rather than round specimens. The stiffening effect of the square overhang is not considered to be significant for either the BOR or ROR specimens;^{5,7} however, in the HB test, an additional hydraulic pressure is applied against the overhang. Thus, in this paper, both square and round specimens are tested.

II. Stress Equations

Using the analysis of Kirstein and Woolley,¹⁴ the following equation⁷ can be used to calculate the maximum stress σ at the center of a BOR test specimen:

$$\sigma = \frac{3P(1+\nu)}{4\pi t^2} \left\{ 1 + 2 \ln \left(\frac{a}{b} \right) + \left[\frac{(1-\nu)a^2}{(1+\nu)R^2} \right] \left[1 - \left(\frac{b^2}{2a^2} \right) \right] \right\} \quad (1)$$

where P is the measured load, ν the Poisson's ratio, t the specimen thickness, a the specimen support radius, R the specimen radius, and b an equivalent radius of constant stress (b has been estimated to be $t/3^{7,8}$).

Shetty *et al.*¹⁰ modified the solution of Roark and Young¹⁵ for a thin elastic disk that was loaded uniformly at the center by considering the stiffening effect of the annular region outside the support ring between $r = a$ and $r = R$, where r is the radial distance to a point on the specimen:

$$\sigma_{\text{radial}} = \frac{3P(1+\nu)}{4\pi t^2} \left[2 \ln \left(\frac{a}{r} \right) + \frac{(1-\nu)}{2(1+\nu)} \left(\frac{a^2 - r^2}{a} \right) \left(\frac{b^2}{r^2} \right) \left(\frac{a^2}{R^2} \right) \right] \quad (2)$$

$$\sigma_{\text{tangential}} = \frac{3P(1+\nu)}{4\pi t^2} \left[2 \ln \left(\frac{a}{r} \right) + \frac{(1-\nu)}{2(1+\nu)} \left(4 - \frac{b^2}{r^2} \right) \left(\frac{b^2}{R^2} \right) \right] \quad (3)$$

K. T. Faber—contributing editor

Manuscript No. 190591. Received November 6, 1997; approved March 23, 1999. Supported by the Center for Ceramic Research and the New Jersey Commission for Science and Education.

^{*}Member, American Ceramic Society.

[†]Now with Ronniger-Petter Engineered Filter Systems, Portage, MI.

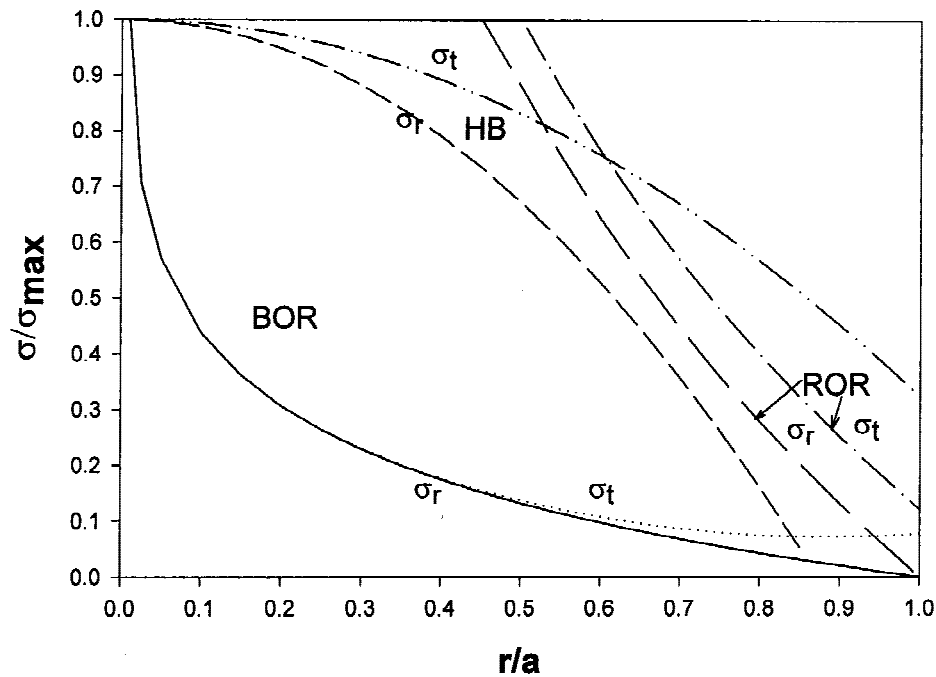


Fig. 1. Calculated radial (σ_r) and tangential (σ_t) stresses for (a) ball-on-ring (BOR) and (b) hydraulic-burst (HB) tests. Dimensions were taken from the samples used in this study: $2a = 20$ mm, $2R = 25$ mm, and $t = 0.635$ mm. The stress within the inside ring during ring-on-ring (ROR) testing is assumed to be constant, as is the stress within the radius b for the BOR test.

The HB test eliminates the very-steep stress gradient that is observed using the BOR technique and results in a more-uniform stress distribution over the disk. Hydraulic pressure is applied via a neoprene diaphragm to one side of a specimen that is resting against a support ring. Mansfield¹⁶ modified the stress calculation of Timoshenko¹⁷ to account for the stiffening effect of the overhang, and Matthewson and Field⁹ further modified the calculation to account for the pressure on the overhang of a circular specimen. Their result is

$$\sigma_r = \frac{3pa^2}{8t^2} \left[2(1-\nu) + (1+3\nu)\left(\frac{R}{a}\right)^2 - 4(1+\nu)\left(\frac{R}{a}\right)^2 \ln\left(\frac{R}{a}\right) - (3+\nu)\left(\frac{r}{a}\right)^2 \right] + \frac{(3+\nu)p}{4(1-\nu)} \quad (4)$$

$$\sigma_t = \frac{3pa^2}{8t^2} \left[2(1-\nu) + (1+3\nu)\left(\frac{R}{a}\right)^2 - 4(1+\nu)\left(\frac{R}{a}\right)^2 \ln\left(\frac{R}{a}\right) - (1+3\nu)\left(\frac{r}{a}\right)^2 \right] + \frac{(3+\nu)p}{4(1-\nu)} \quad (5)$$

where p is the uniform pressure that is applied to the specimen surface.

As shown in Fig. 1, the hoop (tangential) stress (σ_t) is significant at the support distance from the center and at the edge. Thus, support and edge failures cause problems with HB tests. Matthewson and Field⁹ showed that the probability of support and edge failure decreases as the ratio of the support radius to the specimen radius decreases. The contact stresses also increase, because the central stress also decreases and an increase

in pressure is required to maintain the stress level on the specimen. A value of 0.8, which is a compromise for this ratio, was determined experimentally to be satisfactory.

III. Experimental Procedure

(1) Materials

The specimens for the primary portion of the study were high-purity polycrystalline alumina (Al_2O_3) that was obtained from a single lot from a commercial supplier (ADS-996, Coors Ceramic Co., Electronic Div., Golden, CO). The surfaces were as-fired. For both BOR and HB testing, circular and square Al_2O_3 samples with a nominal sample thickness of 0.635 mm were examined. To study the effect of sample size, two sizes of each shape were tested: for square samples, edge lengths of 20 and 25 mm were used, and for circular samples, diameters of 20 and 25 mm were used. The flatness of the Al_2O_3 samples was tested by comparing the specimen thickness between two glass slides with the specimen thickness that was measured directly. The mean warpage value for all the Al_2O_3 samples was 0.015 mm, or $\sim 2\%$ of the nominal thickness, and no correlation was observed between warpage and strength. The specimens were covered by an adhesive, vinyl clean-room tape, to preserve the fracture pattern. All specimens were handled with latex gloves, and no cleaning or other surface preparation was performed.

The second phase of the study investigated the strength distributions of aluminum nitride (AlN) substrates. Three sets of translucent AlN substrates (dimensions of 7.62 cm \times 7.62 cm (3 in. \times 3 in.)) were obtained from several commercial suppliers; the properties of these substrates are shown in Table I.

Table I. Aluminum Nitride Sample Characteristics

Set	Powder process	Color	Density (g/cm ³)	Specimen thickness (mm)	Thermal conductivity (W·(m·K) ⁻¹)
E	Direct nitridation	Gray	2.5–3.3	0.66	228–330
F	Direct nitridation	Gray	2.5–3.3	0.81	215–219
G	Carbothermal reduction	Light tan	3.1–3.3	0.66	124–133

Variation among the three sets is attributed to the powder sources and processing. The samples were diamond machined to the shape of square samples that were 25.4 mm on each side. The thickness of the specimens was measured at the center and at an edge, and the specimens were covered with vinyl tape on one side. The specimens were equally as flat as the Al_2O_3 specimens.

(2) Testing

The BOR test was performed using a ball-bearing race for the support ring. The ball bearings minimized friction between the specimen and the support ring. The BOR apparatus was built from a design of Rhodes.¹⁸ Load was applied using a tungsten carbide (WC) ball that was 10 mm in diameter. The support rings were interchangeable and had diameters of 16 and 20 mm for the 20 mm and 25 mm diameter specimens, respectively. A screw-type universal testing machine was used to apply load to the piston of the BOR apparatus. The load was applied with a crosshead speed of 0.254 mm/min (0.01 in./min). The loading rate was ~15 and 10 MPa/s (maximum stress) for the 20 mm and 25 mm specimens, respectively. The cross head was reversed immediately when failure occurred, to prevent crushing the fractured specimen or the specimen holder.

The HB test fixture has been described by Rhodes *et al.*¹⁸ The specimen is seated on a ledge in a specimen holder that is located beneath the hydraulic chamber. A ring that has been machined to the desired size keeps the specimen in place during testing, with minimum lateral displacement. The specimen is isolated from the fluid reservoir by a neoprene diaphragm that is 1.6 mm thick, to prevent contamination of the fractured fragments.

A high incidence of support failures was observed in the initial test of three specimens from each sample set. The support edge of the specimen holder was covered by a flexible copper washer that was punched from a strip of copper foil 0.05 mm thick, to minimize flatness problems and reduce contact stresses. Al_2O_3 samples were loaded at a constant rate of hydraulic-pressure increase (0.41 MPa/s). The loading rate was 14 and 20 MPa/s (maximum stress) for the 20 mm and 25 mm specimens, respectively. Thus, the stressing rates for the BOR and HB tests were approximately equal. AlN samples fractured too violently when tested at this rate, such that the retaining vinyl-tape layer and the neoprene diaphragm all failed; therefore, they were loaded at a hydraulic-pressure rate of 0.009 MPa/s. Thirty-nine specimens of each type were tested. The sequence of testing samples was random, to eliminate temporal effects of the testing and the test method. Specimen selection of a given type was random for the BOR and HB tests.

The fractured specimens from the BOR test required no re-assembly, because the fracture pattern showed no repeated bifurcation. The localized load at the specimen center resulted in fragments (typically six, which were assembled intact on the vinyl tape). The fracture origin of the HB specimens was much more varied and was never located exactly in the center. Fracture patterns were bifurcated, and pieces frequently shifted or pulled from the vinyl tape. The AlN samples also resulted in bifurcated fracture patterns; however, none of these specimen fragments were displaced greatly. Visual inspection and optical microscopy were used to locate the region of crack origin. Selected samples were examined using scanning electron microscopy (SEM) to identify the fracture origin. The humidity was not controlled; however, no correlation was observed between the strength and the variations in relative humidity

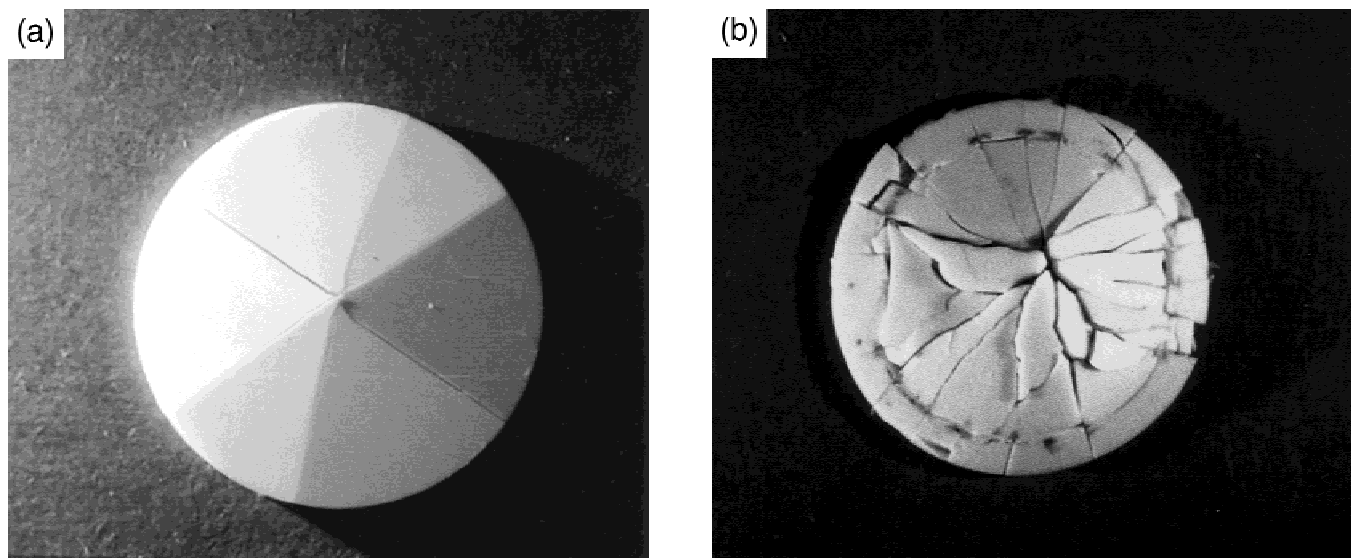


Fig. 2. Typical fracture patterns for (a) ball-on-ring (BOR) and (b) hydraulic-burst (HB) tests.

Table II. Alumina Flexure-Test Results

Sample [†]	Shape	Length (mm)	Mean strength (MPa)	Number of edge failures	Number of support failures
BOR test					
A	Square	20	1064	0	0
B	Circular	20	998	0	0
C	Square	25	894	0	0
D	Circular	25	933	0	0
HB test					
A	Square	20	489	0	3
B	Circular	20	301	4	10
C	Square	25	311	0	5
D	Circular	25	226	1	0

[†]Thirty nine specimens of each sample type were tested.

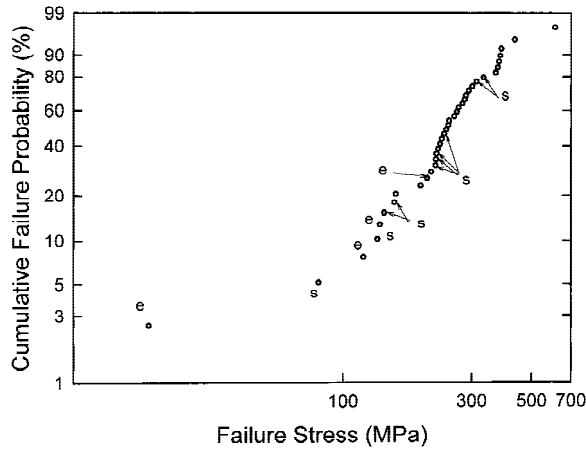


Fig. 3. Weibull strength distribution with flaw locations of Al_2O_3 via HB testing for sample B ("e" denotes edge, and "s" denotes support).

(RH). The mean RH was $\sim 16\%$ and normally over a range of $\sim 10\%$ – 25% .

The HB test was selected to test the flexure strengths of AlN samples. Only square specimens (25.4 mm on a side) were tested. They were diamond cut, and no other polishing or sample preparation was performed for the testing.

IV. Results

(1) Alumina

Fracture patterns for both BOR and HB (square and circular specimens) are shown in Figs. 2(a) and (b), respectively. All BOR failures originated in the center of the circle or square specimen and were less branched than the HB failures. For the HB specimens, the visible cracks in the support ring occurred

after fracture was initiated and were not the failure origins. Secondary cracks were easily identified in samples with obvious fracture origins. These cracks originated after the primary crack initiated specimen failure and rarely were located at the same failure location as the primary cracks. They frequently were identified by crack paths that traversed the primary crack paths. Samples with several sets of multiple secondary cracking required examination via optical microscopy to isolate the primary cracking event. The fracture origins of the BOR specimens were always located at the center, whereas the fracture origins in HB specimens were distributed throughout the sample. The location of the failure origins, relative to the surface, was determined in a few specimens. The origin varied between the bulk, the subsurface,¹⁹ and the surface: the BOR flaws originated at the surface or near the surface, and more HB failures were observed in the bulk.

The results of the BOR and HB biaxial-flexure tests are summarized in Table II and Figs. 3–5. The length parameter in Table II is the edge length for square samples and the diameter for circular samples. The number of edge and support failures from each sample set also is listed in Table II. The edge and support failures, which all were originated in HB tests, were excluded from the mean-strength calculations in Table II. The $\sim 25\%$ edge failures for sample B of the HB test compare with the 5%–15% range that was determined by previous investigators; however, sample D of the HB test exhibited no support failures. Figure 3 shows the Weibull plot for sample B of the HB test, with the edge and support failures included. The break in the curve at low stress is entirely due to edge and support failures. Other edge and support failures seem consistent with the Weibull curve for normal failures.

Figures 4 and 5 show Weibull plots for the fracture of Al_2O_3 specimens, with the edge and support failures eliminated, for BOR and HB tests, respectively. Table III contains Weibull moduli data that have been calculated for the BOR and HB tests, using an unbiased maximum likelihood estimator technique.²⁰ The mean strengths that were determined using the BOR test were 2–4 times higher than those that were deter-

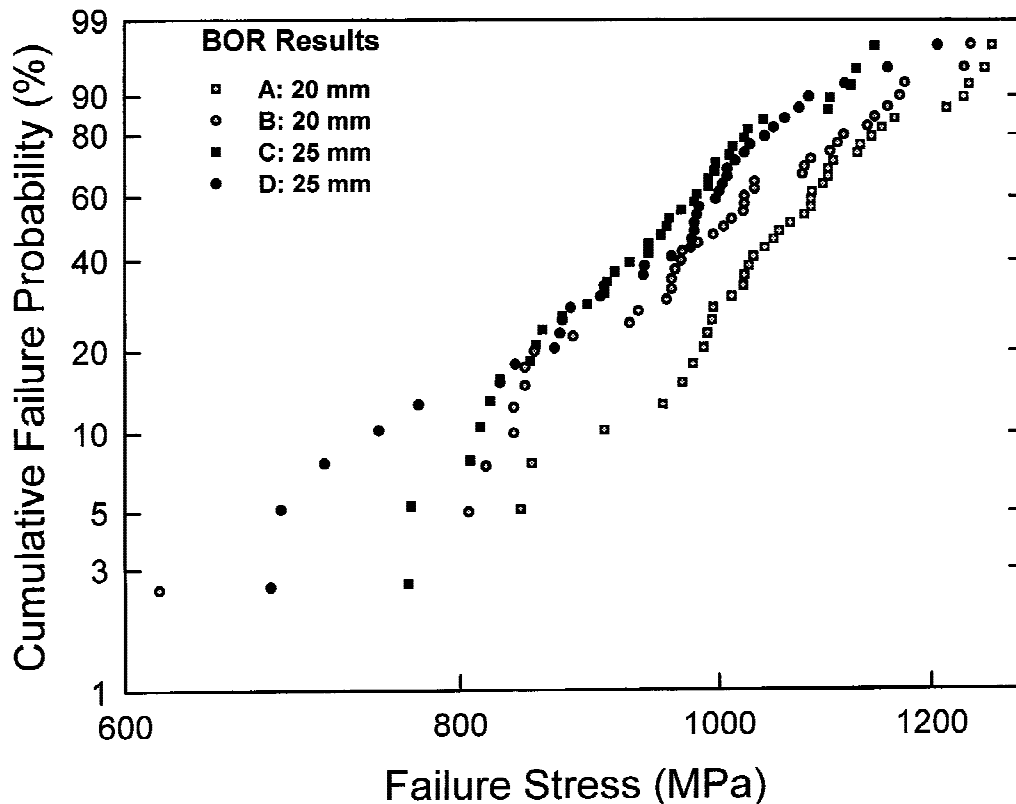


Fig. 4. BOR fracture-strength distribution of Al_2O_3 specimens.

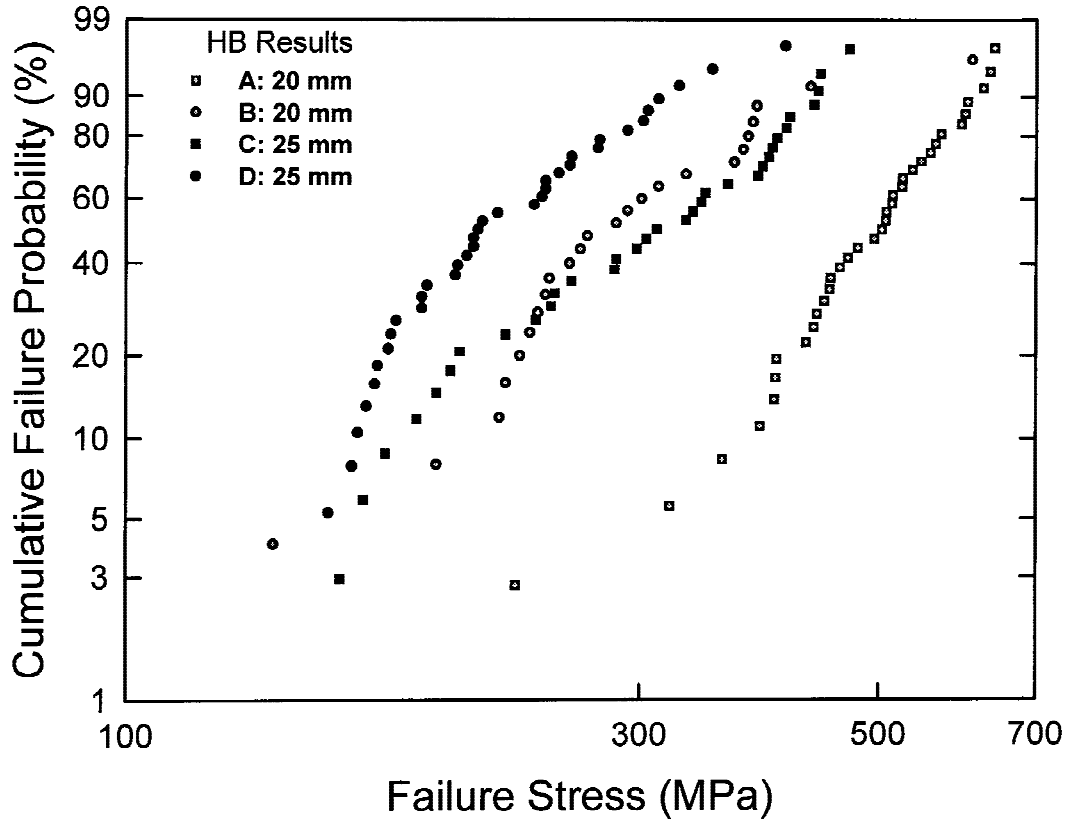


Fig. 5. HB fracture-strength distribution of Al₂O₃ specimens.

mined using the HB test. The *m* values also are higher. Furthermore, the size and shape of the sample makes a greater difference in mean-strength values for the HB test than for the BOR test. These results, presumably, are related to the ability of the HB test to sense a more diverse population of flaws, as discussed later in this paper. Although the location of the fracture origin was identified, the flaw types were not.

(2) Aluminum Nitride

Figure 6 shows the Weibull distributions of the AlN flexure strengths. The mean strengths are shown in Table IV. The majority of the AlN specimens exhibited bulk failures at varying distances from the center. The portion of support failures was approximately the same as that for the Al₂O₃ specimens. Edge failures were more numerous and were attributed directly to the diamond machining that was performed to prepare the samples, which resulted in visibly nonuniform edges. Edge and support failures were eliminated in Fig. 6.

V. Discussion

(1) Hydraulic-Burst versus Ball-on-Ring Testing

Table II indicates that the BOR specimens are much stronger than the HB specimens. To analyze the statistics of specimen size and the effect of stress state and stress variations, both the Weibull²¹ approach and the Barnett-Freudenthal^{1,22} approxi-

mation approach to biaxial stresses were applied. Using two-parameter Weibull statistics and a surface source of flaws, the probability of failure (*P_f*) is

$$P_f = 1 - \exp(-B) \tag{6}$$

where *B* is the risk of rupture, which is defined as

$$B = \int_A \left(\frac{\sigma}{\sigma_o}\right)^m dA = \left(\frac{\sigma_{max}}{\sigma_o}\right)^m 2\pi a^2 L \tag{7}$$

where σ_o is a constant, *A* the area, and *L* the loading factor. *L* accounts for the stress gradient over the area. The term $2\pi a^2 L$ is an effective area when *L* < 1. For a biaxial stress state, Shetty *et al.*¹⁰ showed that *L*, on an area basis, is given by

$$L = \frac{2(2m + 1)}{\pi a^2} \times \int_0^a \left\{ \int_0^{\pi/2} \int_{-\pi/2}^{\pi/2} \left(\frac{\sigma_r}{\sigma_{max}} \cos^2 \psi + \frac{\sigma_t}{\sigma_{max}} \sin^2 \psi \right)^m \times \cos^{2m+1} \phi d\phi d\psi \right\} r dr \tag{8}$$

where ϕ is the out-of-plane angle and ψ is the in-plane angle, relative to the surface of the specimen, in spherical coordinates. To calculate *L* for the BOR test, *B* was divided into two parts—*L_{max}* for *r* < *b* and *L_r* for *a* > *r* > *b*:

$$B = B_{max} + B_r = 2\pi a^2 \left(\frac{\sigma}{\sigma_o}\right)^m (L_{max} + L_r) = 2\pi a^2 \left(\frac{\sigma}{\sigma_o}\right)^m L_{BOR} \tag{9}$$

To calculate *L_{max}*, Eq. (1) is substituted into Eq. (8); to calculate *L_r*, Eqs. (2) and (3) are substituted into Eq. (8). The calculation of *L*, on a volume basis, is similar, except that inte-

Table III. Alumina Flexure-Test Moduli

Sample	Weibull modulus data, BOR test		Weibull modulus data, HB test	
	<i>m</i>	95% limit	<i>m</i>	95% limit
A	9.8	7.6–12.6	6.1	4.6–8.0
B	8.6	6.6–11	3.0	2.1–4.1
C	10.1	7.8–13	3.8	2.8–4.9
D	8.9	6.8–11.4	3.8	2.9–5.0

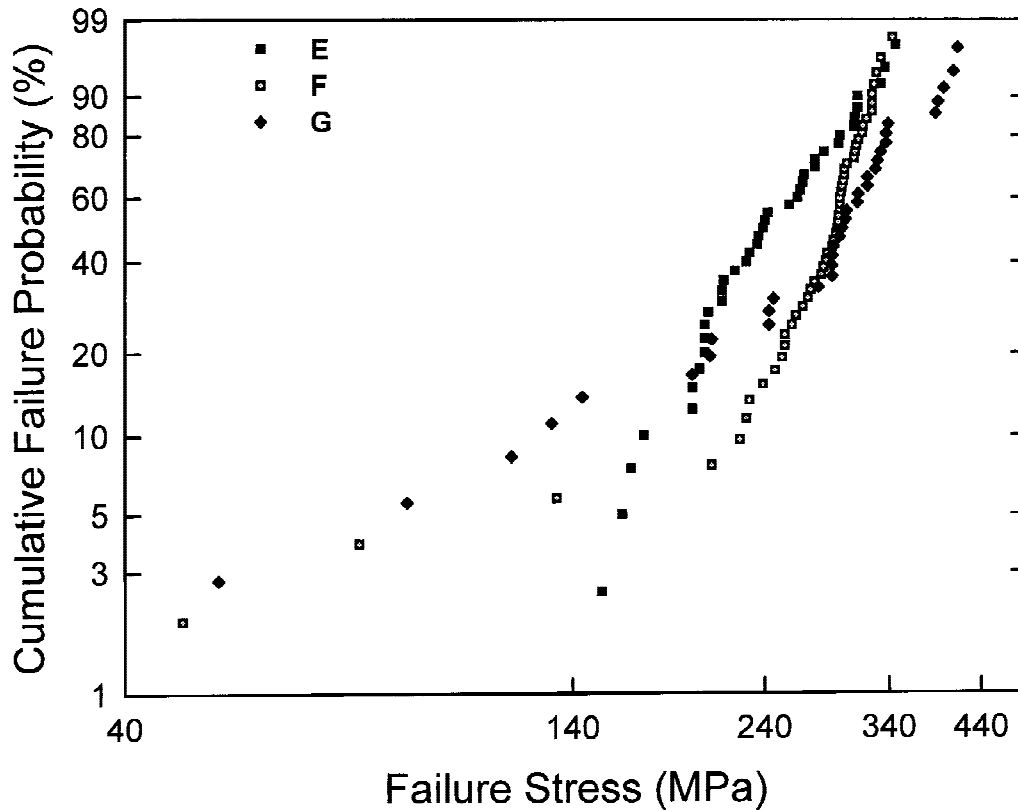


Fig. 6. HB fracture-strength distribution for square AlN specimens.

gration is performed over the tensile volume of the specimen. The results are as follows: $L_{BOR}(\text{volume}) = (L_{BOR}(\text{area}))\{1/(m + 1)\}$ and $L_{HB}(\text{volume}) = (L_{HB}(\text{area}))\{1/(m + 1)\}$. In the Barnett–Freudenthal approximation method, the principle stresses are assumed to act independently; therefore,¹

$$B = 2\pi \int_r \left(\frac{\sigma_r}{\sigma_o}\right)^m r dr + 2\pi \int_r \left(\frac{\sigma_t}{\sigma_o}\right)^m r dr \quad (10)$$

Figure 7 compares the loading factors for the HB and BOR tests, based on area, for two different-sized specimens. The values that have been obtained are consistent with previous literature.²³ Figure 8 clearly shows that L is a function of the Weibull modulus m . Given an m value of ≥ 5 , L , based on area, for the BOR test is 0.001–0.01, whereas that for the HB test remains >0.5 .

The ratio of the loading factors (L_{HB}/L_{BOR}) is plotted in Fig. 8 as a function of m . This ratio passes through a maximum at $m = 14$. The maximum occurs because, at small m values, L_{HB} decreases much more slowly than does L_{BOR} ; however, as m approaches infinity, L_{BOR} approaches b^2/a^2 , whereas L_{HB} approaches zero. Actually, this observation is only an artifact of Eq. (2), which assumes that the stress is constant within the radius b , which is not true; therefore, the ratio, in fact, may exceed 300.

The ratios of the loading factors, as shown in Fig. 8, are interesting to examine because they represent not only the ratio of effective stressed areas but also may be considered as the

number of BOR specimens that are required to test the same stressed area or volume as one HB specimen. That is, for $m = 14$, 300 BOR specimens must be tested to determine the equivalent number of severe flaws that are observed in one HB specimen. Thus, to obtain the number of BOR data points that is equivalent to the 39 HB data points ($m = 3.8$), 2106 BOR specimens must be tested. This task is not feasible; therefore, there is considerable motivation for testing specimens using the HB or ROR tests, where a large area of the specimen is stressed near the maximum stress.

Because each HB test can be considered to represent 54 BOR tests ($m = 3.8$), the HB results may be considered as being representative of the low-stress portion of the BOR distribution. It is possible to translate the HB distribution vertically downward and plot it on the same graph with the BOR

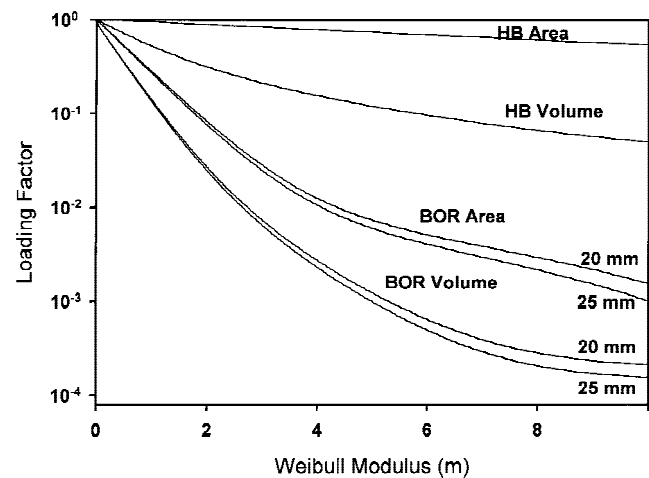


Fig. 7. Comparison of loading factors for BOR and HB tests.

Table IV. Aluminum Nitride Flexure Strengths

Set	Number of samples	Flexure strength (MPa)	Weibull modulus, m	Number of edge failures	Number of support failures
E	47	245	4.0	5	3
F	55	276	5.9	2	2
G	50	279	3.4	4	5

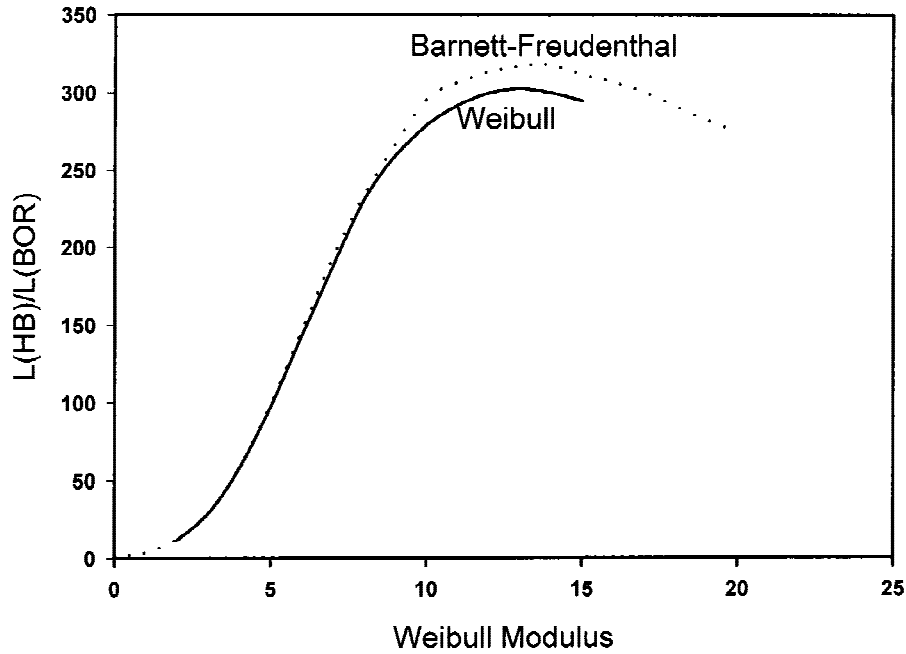


Fig. 8. Ratio of loading factors (L_{HB}/L_{BOR}), as a function of the Weibull modulus.

data. This translation is performed by determining the equivalent P_f^{BOR} value, from Eq. (11):

$$\ln \left[\ln \left(\frac{1}{1 - P_f^{BOR}} \right) \right] = \ln \left[\ln \left(\frac{1}{1 - P_f^{HB}} \right) \right] - \ln \left(\frac{L_{HB}}{L_{BOR}} \right) \quad (11)$$

Figure 9 shows such a plot for the circular Al_2O_3 specimens 25 mm in diameter; these data were determined by substituting L_{HB} ($m = 3.8$) and L_{BOR} ($m = 8.9$) in Eq. (11). These are appropriate choices for L_{HB} and L_{BOR} , because if they were both referenced to pure biaxial tension ($L = 1$) rather than to BOR testing, the same relative positions of the strength distributions would be obtained. Notably, more of the flaws in the HB tests were volume flaws, whereas in the BOR test, most were surface or near-surface flaws; therefore, both $L_{HB}(\text{area})$ and $L_{HB}(\text{volume})$ were considered in Fig. 9. In both cases, the HB data in Fig. 9 seem to be a low-strength continuation of the BOR data. The excellent fit of both curves gives support to both the stress and loading-factor calculations. The changing slope in going from the BOR data to the HB tail indicates a

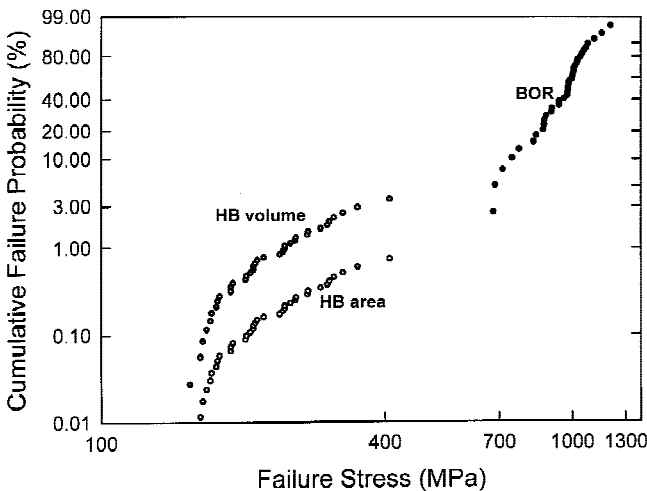


Fig. 9. BOR fracture-strength distribution with HB data superimposed by shifting the HB data vertically, according to Eq. (10).

change in fracture origin. The Weibull modulus m of the tail must be smaller, because, for two different flaw-size distributions, the larger flaw must dominate. More of the HB flaws were observed in the volume; therefore, these flaws likely have different origins and possess different size distributions. On the other hand, the area curve for HB testing is more continuous with the BOR data.

(2) Specimen Size and Shape

Table II shows that, in each case, the 25 mm specimens had a smaller mean strength than did the 20 mm specimens. Table V compares the $[(L_1 a_1^2)/(L_2 a_2^2)]^{1/m}$ ratios for the 20 mm (L_2) and 25 mm (L_1) specimens with the inverse ratios of the mean strengths. The $\bar{\sigma}_2/\bar{\sigma}_1$ ratios are much higher for both the BOR and HB tests than those predicted by the $[(L_1 a_1^2)/(L_2 a_2^2)]^{1/m}$ ratios, which indicates that size differences may not be fully considered by the loading factor L , especially in the HB data.

According to Fig. 5, square HB samples have a higher mean strength than do circular specimens for both sample diameters. The greater overhang of the square specimens, which is due to their corners, must contribute to the strengthening. The effect was strongest with the small specimens (sample A vs sample B), where the increase in strength, from circular to square geometries, was 62%, compared to 37% for the larger specimens (see Table II). Also, according to Table III, there is a significant difference in the apparent Weibull modulus. The stiffening effect reduces the circumferential stress near the edge, as evidenced by the fact that no edge failures occurred on the square specimens. The overlap effect for the square is strongest for the smaller-diameter specimens. Because the

Table V. Comparison with Experimental and Weibull Size Factors

Sample	$\bar{\sigma}_2/\bar{\sigma}_1$	$[(L_1 a_1^2)/(L_2 a_2^2)]^{1/m^\dagger}$
BOR test		
A/C	1.19	1.006
B/D	1.07	1.006
HB test		
A/C	1.57	1.09
B/D	1.33	1.12

[†]Values of m were taken as the average of the m values given in Table II.

mean measured strength of the larger square specimens is similar to that of the circular specimens, and because Eqs. (4) and (5) describe the stress state of the circular specimens in the HB test, the larger square specimens presumably better approximate the calculated stress state. In the previous study by Matthewson and Field,⁹ the optimum a/R ratio was estimated to be 0.8. Both specimen sizes used an a/R ratio of 0.8 in the current study; therefore, it must be concluded that the magnitude of a for square specimens also is important. The optimum-sized square specimen has not been determined as part of this study.

VI. Conclusions

Rather than perform a prohibitively large number of ball-on-ring (BOR) tests to determine if the low-stress tail exhibited a different Weibull modulus (m) than the high-stress portion, hydraulic-burst (HB) tests were performed. The justification was that the HB tests sampled a much-larger stressed area (stressed volume) than did the BOR tests and, therefore, could be considered as being equivalent to testing several BOR specimens. This observation was evidenced by plotting both HB and BOR data on the same graph and using the loading factor (L) to shift the HB data into the relative position that was predicted by L . The result was that, indeed, the lower HB portion fit well as a continuation of the BOR data and exhibited a different m value. The implication is that if the BOR test is used to determine whether a given set of processing conditions has improved the strength, it may have only improved one set of flaws and not the flaws of the low-strength tail. Therefore, the use of either HB or ring-on-ring (ROR) tests is highly recommended for this purpose.

In addition, this study supports earlier observations that edge and support failures are more prevalent in HB testing than in BOR testing; however, even if these data are eliminated, this flaw concentration only slightly increases the number of tests that are required. This condition does require that fracture analysis be performed on all specimens, to eliminate edge and support failures. Despite this problem, the HB test is preferred over the BOR test, for the above-mentioned reasons; however, the ROR test may be a better alternative for square specimens.

Finally, this study indicates that variation in the size and shape of the HB specimens caused larger changes in strength values for the HB test than for the BOR test. This study did not determine the optimum size for either the circular or square specimens; however, it did indicate that the larger, 25 mm diameter, square specimens would be preferred over the smaller, 20 mm diameter, specimens.

References

- ¹D. K. Shetty, A. R. Rosenfeld, and G. K. Bansal, "Biaxial Studies of a Glass-Ceramic," *J. Am. Ceram. Soc.*, **64** [1] 1–4 (1981).
- ²L.-Y. Chao and D. K. Shetty, "Reliability Analysis of Structural Ceramics Subjected to Biaxial Flexure," *J. Am. Ceram. Soc.*, **74** [2] 333–44 (1991).
- ³R. Thiruvengadswamy and R. O. Scattergood, "Biaxial Flexure Testing of Brittle Materials," *Scr. Metall.*, **25**, 2529–32 (1991).
- ⁴J. B. Wachtman, W. Capps, and J. Madel, "Biaxial Flexure Tests of Ceramic Substrates," *J. Mater.*, **7** [2] 88–94 (1972).
- ⁵J. E. Ritter Jr., K. Jakus, A. Batakis, and N. Bandyopadhyay, "Appraisal of Biaxial Strength Testing," *J. Non-Cryst. Solids*, **38&39**, 419–24 (1980).
- ⁶H. Fessler and D. C. Fricker, "A Theoretical Analysis of the Ring-on-Ring Loading Disk Test," *J. Am. Ceram. Soc.*, **67** [9] 582–88 (1984).
- ⁷D. K. Shetty, A. R. Rosenfeld, P. McGuire, G. K. Bansal, and W. H. Duckworth, "Biaxial Flexure Test for Ceramics," *Am. Ceram. Soc. Bull.*, **59** [12] 1193–97 (1980).
- ⁸G. de With and H. H. M. Wagemans, "Ball-on-Ring Revisited," *J. Am. Ceram. Soc.*, **72** [8] 1538–41 (1989).
- ⁹M. J. Matthewson and J. E. Field, "An Improved Strength-Measurement Technique for Brittle Materials," *J. Phys. E: Sci. Instrum.*, **13**, 355–59 (1980).
- ¹⁰D. K. Shetty, A. R. Rosenfeld, W. H. Duckworth, and P. R. Held, "A Biaxial-Flexure Test for Evaluating Ceramic Strengths," *J. Am. Ceram. Soc.*, **66** [1] 36–42 (1983).
- ¹¹C. R. Kurkjian, R. V. Abarino, J. T. Krause, H. N. Vazirani, F. V. DiMarcello, S. Torza, and H. Schonhorn, "Strength of 0.04–50-m Lengths of Coated Fused Silica Fibers," *Appl. Phys. Lett.*, **28** [10] 588–90 (1976).
- ¹²D. B. Marshall, "An Improved Biaxial Flexure Test for Ceramics," *Am. Ceram. Soc. Bull.*, **59** [5] 551–53 (1980).
- ¹³W. F. Adler and D. J. Mihora, "Biaxial Flexure Testing: Analysis and Experimental Results"; pp. 227–45 in *Fracture Mechanics of Ceramics*, Vol. 10, *Fracture Fundamentals, High-Temperature Deformation, Damage, and Design*. Edited by R. C. Bradt, D. P. H. Hasselman, D. Munz, M. Sakai, and V. Ya. Shevchenko. Plenum Press, New York, 1992.
- ¹⁴A. F. Kirstein and R. M. Woolley, "Symmetrical Bending of Thin Circular Elastic Plates on Equally Spaced Point Supports," *J. Res. Natl. Bur. Stand., Sect. C*, **71C** [1] 1–10 (1966).
- ¹⁵R. J. Roark and W. C. Young, *Formulas for Stress and Strain*. McGraw-Hill, New York, 1975.
- ¹⁶E. H. Mansfield, "The Stiffening Effect of an Overhang in a Circular Plate," *J. R. Aeronaut. Soc.*, **67**, 671–72 (1963).
- ¹⁷S. Timoshenko, *Theory of Plates and Shells*. McGraw-Hill, New York, 1940.
- ¹⁸W. H. Rhodes, M. R. Pascucci, G. C. Wei, E. A. Trickett, S. Natansohn, C. Brecher, and F. J. Avella, "Development of Lanthanum-Doped Ytria as an Optical Ceramic," NWC Rept. No. TR-001-88-878, pp. 47–56, Naval Weapons Center, 1988.
- ¹⁹A. G. Evans and G. Tapin, "Effects of Microstructure on the Stress to Propagate Inherent Flaws," *Proc. Br. Ceram. Soc.*, **20**, 275–97 (1972).
- ²⁰D. R. Thoman, L. J. Bain, and C. E. Antle, "Inferences on the Parameters of Weibull Distribution," *Technometrics*, **11**, 445–60 (1969).
- ²¹W. Weibull, "A Statistical Theory of the Strength of Materials," *Ingenjersvetenskapsakad. Handl.*, **151**, 1–45 (1939).
- ²²R. L. Barnett, P. C. Hermann, J. R. Wingfield, and C. L. Connors, "Fracture of Brittle Materials under Transient Mechanical and Thermal Loading," Rept. No. TR-66-220. Air Force Flight Dynamics Laboratory, Dayton, OH, 1967.
- ²³K. C. Radford and F. F. Lange, "Loading (L) Factors for the Biaxial Flexure Test," *J. Am. Ceram. Soc.*, **61** [5–6] 211–13 (1978). □